

The enhanced anodic performance of highly crimped and crystalline nanofibrillar carbon in lithium-ion batteries

Hyeon Gu Cho^a, Young Jeon Kim^a, Yung-Eun Sung^b, Chong Rae Park^{a,*}

^a Carbon Nanomaterials Design Laboratory, Hyperstructured Organic Materials Research Center (HOMRC) and Department of Materials Science and Engineering, Seoul National University E445-F, Seoul 151-744, Republic of Korea

^b School of Chemical & Biological Engineering, Seoul National University, Seoul 151-744, Republic of Korea

Received 14 June 2007; received in revised form 1 August 2007; accepted 1 August 2007

Available online 7 August 2007

Abstract

To find a novel high-performance anode material for lithium-ion batteries, a new form of carbon characterized by highly crimped and crystalline nanofibrillar microtextures was produced by heat treating polyacrylonitrile/FeCl₃ hybrid precursor and subsequent thermal annealing under hydrogen gas. This form of carbon exhibits a rechargeable capacity of ~630 mAh/g, which is superior to that of graphite, with a Coulomb efficiency of ~70%. Further, the new form of carbon was found to exhibit an efficiency of lithium ion insertion/extraction of ~100% in the voltage range from 0.06 to 0.80 V, with a capacity of ~400 mAh/g. We speculate that this excellent capacity is due to the characteristic structure of this form of carbon, i.e. its highly entangled web-like hyperstructure consisting of highly crimped and crystalline nanofibrillar microtextures, which enables good permeation and has high resilience to volume deformation during the insertion/extraction of Li ions.

© 2007 Elsevier Ltd. All rights reserved.

Keywords: Highly crimped and crystalline carbon; Nanofibrils; Transmission electron microscopy; Electrochemical performance; Li-ion battery

1. Introduction

During the last decade, the possible applications in many areas of various carbon nanomaterials such as nanotubes and buckyballs [1,2] have been extensively explored [3–5]. For example, carbon nanotubes have been suggested as good candidates for anode materials in Li-ion batteries (LIBs) [6] since they have many available sites for the adsorption of Li ions including the outer and inner surfaces of the graphene rolls, and the interlayers between the graphene sheets in the case of multi-wall nanotubes. However, tip-opened nanotubes have a large irreversible capacity, 941 mAh/g, which is the difference between the charge capacity, 1281 mAh/g, and the discharge capacity, 340 mAh/g [7]. This result indicates that the anodic performance of carbon materials in lithium-ion batteries (LIBs) is not a simple function of the number of available sites for the adsorption of lithium ions. Thus, to develop high-performance anodic carbon materials, other factors must also be considered,

such as the energy barrier to the Li-ion insertion/extraction process, the volume deformation of the carbon anodes during this process, and the lengths of the diffusion paths of the Li ions.

The microtexture of natural cotton consists of highly crimped and crystalline ribbon-like strands called microfibrils that are 10–20 nm in width. The crimped and crystalline ribbon-like strands form fibers that make up a web-like hyperstructure. This kind of microstructure exhibits good permeation and high resilience to volume deformation. We attempted to fabricate carbon with such a microstructure so as to mimic that of natural cotton by producing highly crimped and crystalline carbon nanofibrils that correspond to the microfibrils of natural cotton. The carbon nanofibrils are expected to directly assemble into a web-like open framework. Because of the microtextural similarities of natural cotton and the new form of carbon, we refer to the new form of carbon as carbon-cotton. With these structural characteristics, carbon-cottons are expected to have significant advantages as anodic materials in lithium-ion batteries: easy accessibility to Li ions through the web-like open framework structure, good recovery from volume deformation during the Li-ion insertion/extraction process, and very stable charge–discharge cycleability due to the highly crimped and

* Corresponding author. Tel.: +82 2 880 8030; fax: +82 2 885 1748.

E-mail address: crpark@snu.ac.kr (C.R. Park).

crystalline nanofibrils, which shorten the diffusion paths of the Li ions [8,9]. It is well known that considerable volume changes occur in anodic carbon during the insertion/extraction of Li ions, which are detrimental to the performance of lithium-ion batteries (LIBs).

We report an easy fabrication method, the microstructural characteristics, and the enhanced electrochemical anodic performance of this new ‘carbon-cotton’ carbon. We fabricated carbon-cotton from polyacrylonitrile (PAN)/FeCl₃ hybrid precursor after careful carbonization under nitrogen atmosphere and subsequent annealing under H₂ gas. Carbon-cotton was found to have a rechargeable capacity of ~630 mAh/g with a Coulomb efficiency of ~70%. In particular, carbon-cotton was found to exhibit an efficiency of lithium ion insertion/extraction of ~100% in the voltage range from 0.06 to 0.80 V with a capacity of ~400 mAh/g.

2. Experimental

Carbon-cotton was prepared by heat treating a polyacrylonitrile (PAN)/FeCl₃ hybrid precursor. To prepare the hybrid precursor, PAN consisting of 91.5 wt% acrylonitrile and 8.5 wt% methylacrylate (Hanil Synthetic Fiber, Korea) was dissolved thoroughly in dimethyl formamide (DMF, 99%, Daejong, Korea), and then mixed with FeCl₃ (97%, Fluka, USA) pre-dissolved in DMF with a mole ratio of [C≡N/FeCl₃]=2. The mixture solution was cast into a film on a glass plate and vacuum dried at 55 °C for 48 h to obtain the PAN/FeCl₃ (2:1) hybrid. The hybrid was then carbonized at 1100 and 1500 °C with a heating ramp of 2 °C/min in N₂ atmosphere (denoted CC1100 and CC1500, respectively). During the heat treatment, iron oxide is formed *in situ* from the reaction between iron and the coordinated DMF molecules [10]. To remove the iron oxide, the carbon-cottons were treated with 5 mol% HCl for 1 day at 50 °C. After thorough washing with methanol, the samples were vacuum dried at 50 °C overnight. Then, to increase the crystallinity, the iron oxide free carbon-cotton was annealed at 800 °C (denoted CC1500A) with H₂ gas purging [11].

The microtexture of the carbon-cotton was investigated with high resolution transmission electron microscopy (HRTEM, JEM-3000F, JEOL, Japan) operating at 300 kV. The degree of crimping, C (%), of the carbon nanofibrils was estimated using an image analysis program (Image-Pro Plus 4.5 software by Media Cybernetics, Silver Spring, MD). In order to monitor the changes in pore characteristics with carbonization temperature, N₂ adsorption–desorption isotherms were recorded at 77 K on a volumetric adsorption instrument (ASAP 2010, Micromeritics, USA) in the relative pressure range from 10⁻⁶ to 1 bar. Prior to the measurements, all the samples were degassed at 250 °C under N₂ flow for at least 3 h. For the electrochemical performance tests, the powdered carbon-cotton samples were well mixed with denka black as a conducting agent and polyvinylidene fluoride (PVdF) dissolved in *N*-methyl pyrrolidone (NMP) as a binder, with a mass ratio of 8:1:1 to form a slurry. The slurry was coated onto a copper foil and then pressed and dried at 120 °C for 4 h under vacuum. A laboratory-made, coin type, electrochemical cell was used with lithium foil as a counter electrode and

1 M LiPF₆ in a mixed solvent of ethylene carbonate and diethylene carbonate (EC + DEC, 1:1, v/v, Cheil Industry, Korea) was used as the electrolyte. Cell assembly and all electrochemical tests were conducted in an argon-filled glove-box. Charge (Li insertion)–discharge (Li extraction) experiments were performed galvanostatically at a current density of 30 mA/g.

3. Results and discussion

3.1. Microstructure of carbon-cotton

The preparation of carbon-cotton is very simple, and was carried out through the carbonization of the PAN/FeCl₃ hybrid precursor at 1100 °C (CC1100) and 1500 °C (CC1500). To increase the crystallinity of the carbon-cotton, the CC1500 sample was annealed at 800 °C (CC1500A) with H₂ gas purging.

Fig. 1(a)–(d) shows the microtextural features of the carbon-cottons. Fig. 1(a) shows the highly crimped web-like open framework structure of CC1100, which is very similar to that of natural cotton. In the representative TEM image of CC1100 in Fig. 1(b), we can see that the carbon nanofibrils have regular thicknesses of approximately 5–15 nm and are highly entangled to form a web-like open framework structure in which mesopores of relatively uniform size are present. The thicknesses of the carbon nanofibrils tend to increase, i.e. from approximately 5–15 nm to approximately 15–20 nm, with increases in the heat treatment temperature (see Fig. 1(c) and (d)). The mechanism for the formation of the carbon nanofibrils is not clear at this stage, but since a catalyst mediates the carbonization process, it is assumed to be similar to the fabrication processes for carbon nanotubes and catalytic carbons [12–14]. Note however that carbon nanotubes form from free C⁺ species in a gas phase reaction catalyzed by iron particles, whereas catalytic carbons form as a result of the solid-state carbonization of precursor/catalyst mixtures. In the case of carbon-cotton, the iron oxides formed *in situ* are catalysts for the carbonization of the hybrid precursor, i.e. polyacrylonitrile (PAN)/FeCl₃ [10].

To characterize the degree of crimping of the carbon nanofibrils (C (%)), the following equation was devised:

$$C(\%) = \frac{l_c - l}{l_c} \times 100 \quad (1)$$

where l is the average value of the end-to-end distance of an individual crimped nanofibril and l_c is the average value of the contour lengths of the nanofibrils located within a 100 nm square grid. For the carbon nanofibrils, C (%) is ~40%, which is much higher than the value of ~10% usually obtained for carbon nanofibers and nanotubes. Such a high value of C (%) is comparable to that for carbon black, which has a highly crumpled sheet-like structure. However, it is important to note that carbon-cotton has an open framework structure formed by the entanglement of highly crimped nanofibrils, whereas carbon blacks have closed cellular compartments [13].

High resolution TEM lattice images of the carbon-cottons show that the carbon nanofibrils in CC1100 consist of poorly packed highly meandering carbon layers (Fig. 2(a)). With increases in the carbonization temperature, relatively well

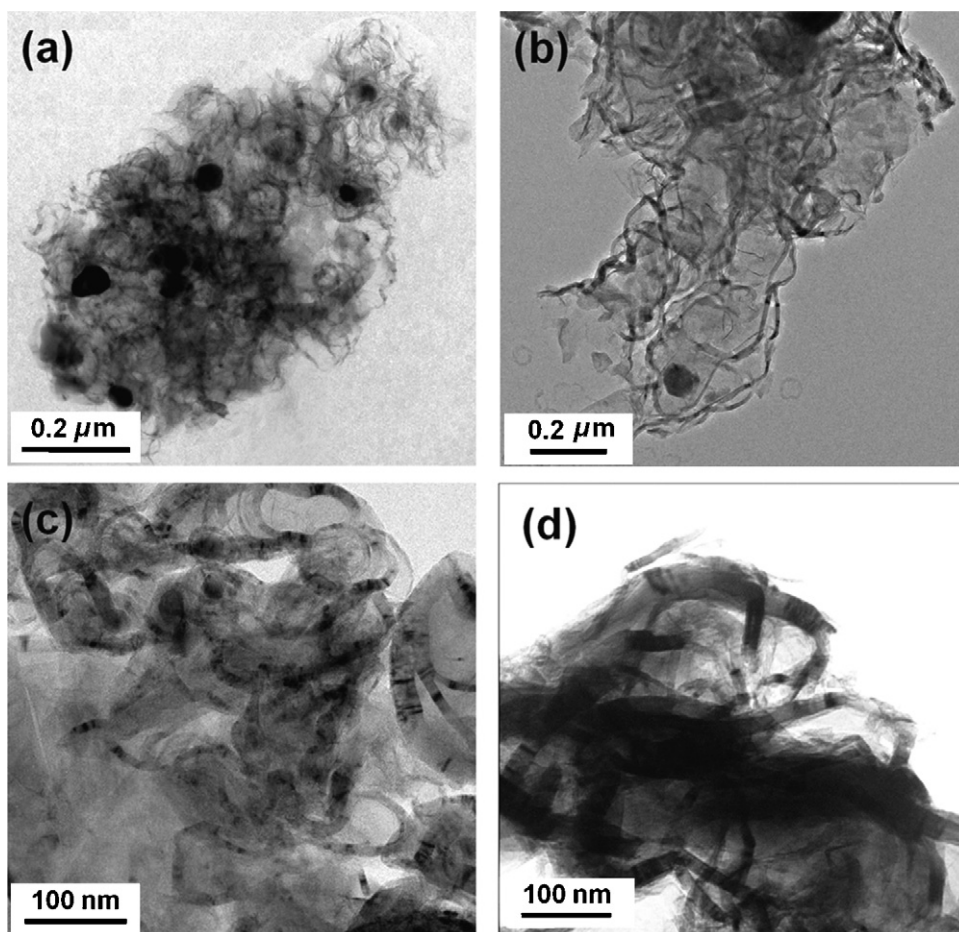


Fig. 1. TEM micrographs of CC1100, CC1500, and CC1500A: (a) debris from a wad of CC1100, (b) an edge region of a wad of CC1100, and edge regions of (c) a wad of CC1500, and (d) a wad of CC1500A.

packed and less meandering carbon layers develop, as can be seen in Fig. 2(b), but structural defects, such as poor packing of the carbon layers and many edges with still underdeveloped carbon layers, are present. It has been suggested that such structural defects are responsible for increases in the irreversibility of the charge/discharge process of Li ions in lithium-ion batteries [15]. To remove these structural defects and hence to improve anodic performance, CC1500 was further thermally annealed at 800 °C under H₂ gas to produce CC1500A. Fig. 2(c) clearly shows that the carbon nanofibrils in CC1500A have drastically improved structures, i.e. they consist of nearly ideally packed (indicated by the interlayer distance of 0.335 nm, which is the value for perfect graphite) and linearly developed graphene layers. It is worth mentioning that the annealing process facilitated more lengthwise structural development than thickness-wise development without significantly affecting the entangled web-like open framework structure. This structural feature might result in both a high Li-ion storage capacity between the graphene layers and a reduction in the lengths of the lateral diffusion paths of the Li ions.

Because of the entanglement of the carbon nanofibrils, pores of various sizes are present in these structures. Indeed, the analysis of the N₂ adsorption/desorption isotherms showed that the

average pore diameter is 60 nm for CC1100 and CC1500 and 6 nm for CC1500A, with BET surface areas of 176, 200, and 244 m²/g, respectively.

3.2. Anodic performance of the carbon-cottons

To test the anodic performance of the carbon-cottons in lithium-ion batteries, the catalyst, i.e. the iron oxide formed *in situ*, was first removed from all the samples with HCl solution, since iron compounds are known to undergo irreversible reactions with Li ions.

The charge–discharge characteristics were measured with the constant-current method and are presented in Fig. 3. Both the charge/discharge capacity and charge profile of CC1500A are distinctively different from those of CC1100 and CC1500: CC1500A exhibits a very good rechargeable capacity of ~630 mAh/g with a Coulomb efficiency of ~70%. This is in strong contrast to the reported electrochemical performance of a carbon black that exhibited a high initial discharge capacity of 912 mAh/g, but exhibited a drastic capacity decay after only the 2nd cycle to 244 mAh/g, with a very low Coulomb efficiency of ~23% [16]. The excellent anodic performance of this carbon-cotton arises possibly because Li ions can diffuse more easily in

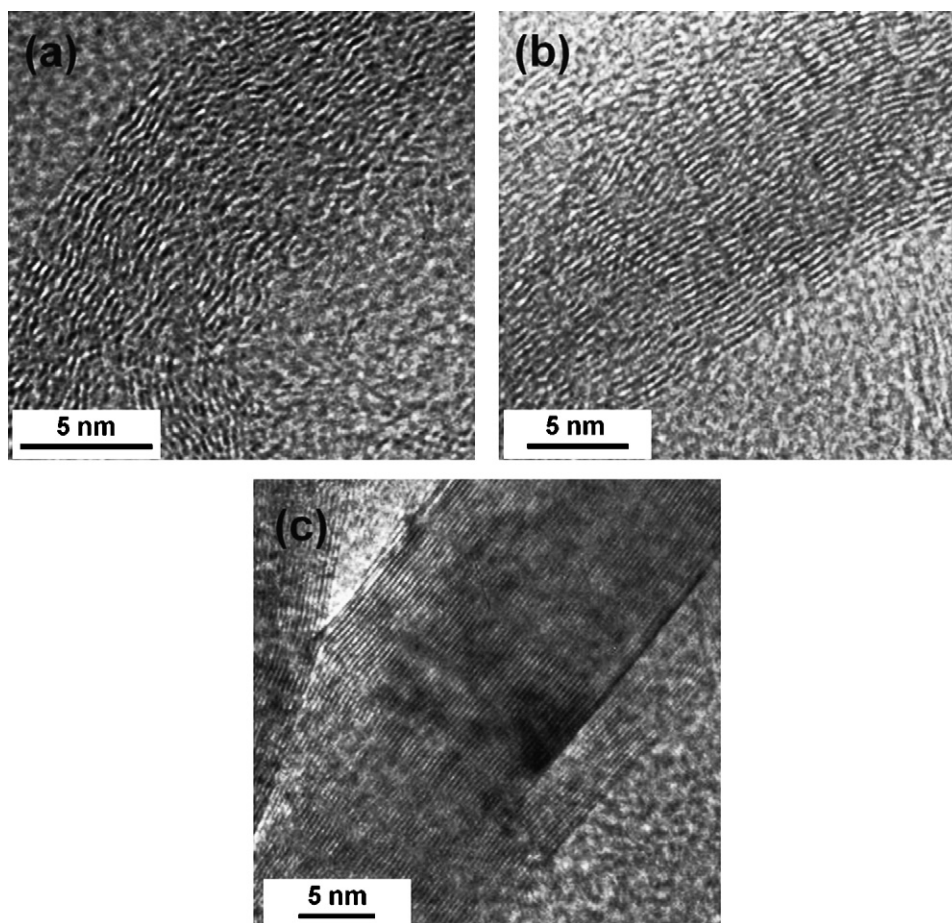


Fig. 2. HRTEM micrographs of the carbon nanofibrils in (a) CC1100, (b) CC1500, and (c) CC1500A.

and out of the web-like open framework structure of the carbon-cotton than is possible for the closed cellular compartments of carbon black.

The differential capacity plots for CC1100, CC1500, and CC1500A provide a more detailed analysis of the charge/discharge behavior, and are shown in Fig. 4. There are some immediately recognizable differences between the Li-ion insertion/extraction behaviors of the samples. During the Li-ion insertion process, the peak at 1.4 V appears only for CC1100, and the peak at 0.8 V is very sharp for CC1100, very broad for CC1500 and very weak for CC1500A. Further, many peaks appear in the range 0.06–0.8 V for CC1100, but there are only two peaks for both CC1500 (at 0.06 and 0.25 V) and CC1500A (at 0.06 and 0.12 V). Note that the peak at 0.25 V for CC1500 is present at 0.12 V after thermal annealing, i.e. for CC1500A. The peak at ~ 0.01 V is common to all samples. During the Li-ion extraction process, there is a broad peak at 0.1 V for CC1100 and CC1500, whereas this peak appears at 0.3 V for CC1500A.

A previously suggested mechanism for Li insertion/extraction [15–18] in carbon anodes indicates that Li ions can be stored at various sites, such as between the carbon layers, in the micropores, on the carbon layer surface, and in the structural defects. During the insertion of Li ions, (i) irreversible reactions between Li ions and electrolytes occur at ~ 0.8 V on the carbon surface and (ii) the intercalation

of Li ions between the carbon layers occurs at 0.25–0.8 V (for graphite). This intercalation process is influenced by the structural characteristics of the carbon material. Further, (iii) Li ions diffuse into the pores at ~ 0.0 V through charge transfer and/or adsorption onto the graphene surface, including onto surface functional groups, H atoms at the edge, and structural defects including heteroatoms. During the extraction of Li ions, Li ions diffuse out of (i) the pores at ~ 0.0 V, (ii) the in-between carbon layers at 0.25–0.8 V, and (iii) the graphene surface, the structural defects, and so on, above 0.8 V.

According to this mechanism, the peaks in Fig. 4 at about 0.8 V for the CC1100 and CC1500 samples are due to an irreversible reaction between Li ions and the electrolyte on the carbon surface. Note that this peak is negligible for CC1500A. Note also that there are many peaks in the voltage range from 0.06 to 0.80 V for CC1100 whereas there are two peaks for both CC1500 and CC1500A but at different voltages. This result indicates that there are many intercalation processes in the case of CC1100, but that the intercalation processes in CC1500 and CC1500A occur in two stages. The voltage for intercalation is lower in CC1500A (0.12 V) than in CC1500 (0.25 V), which suggests that the barrier energy for intercalation is much lower in CC1500A; this difference might be due to the presence of a reduced number of edges of carbon layers in the well-developed crystalline microtexture of CC1500A.

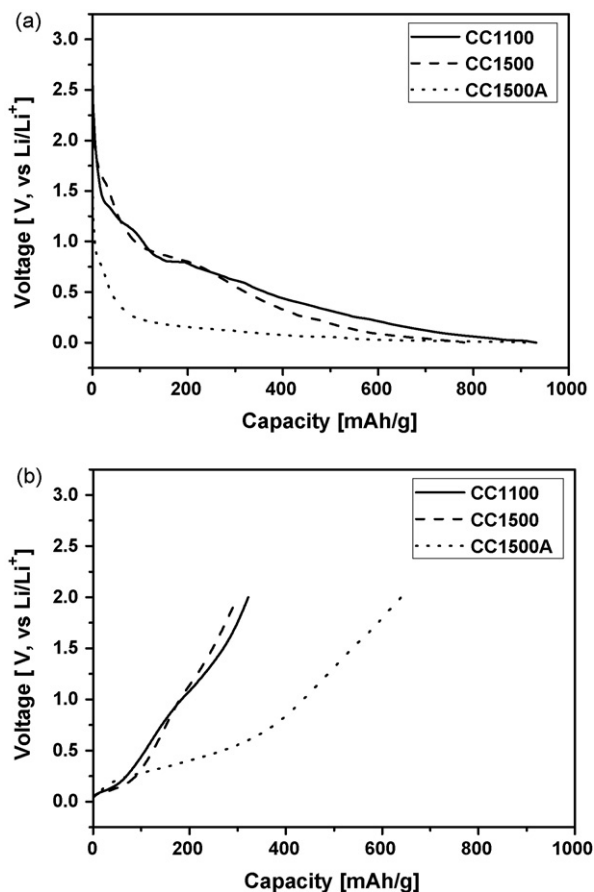


Fig. 3. The first constant-current (a) charging and (b) discharging curves for CC1100, CC1500, and CC1500A.

The charge capacities of all samples in this voltage range, i.e. 0.06–0.80 V, are ~ 400 mAh/g. The peak at 1.40 V is present only for CC1100, and corresponds to a charging capacity of approximately 130 mAh/g, but this is irreversible capacity that possibly arises from the reaction between Li ions and residual Fe species in the sample. Indeed, for this particular sample, it was very difficult to remove the iron oxides completely, because the iron oxide aggregates incorporated well inside the structure did not

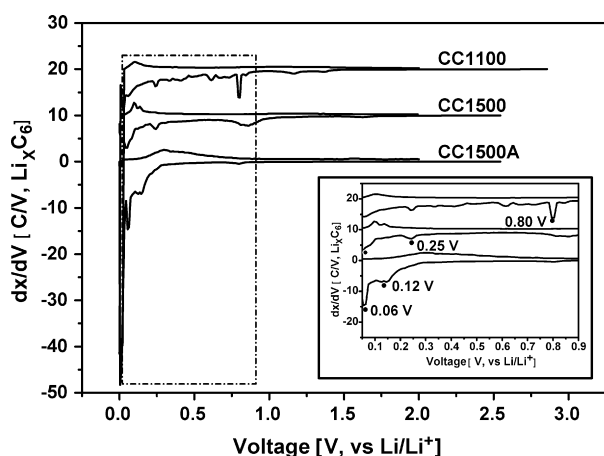


Fig. 4. Differential capacity plots for CC1100, CC1500, and CC1500A. The inset is a magnified plot of the range 0.05–0.90 V.

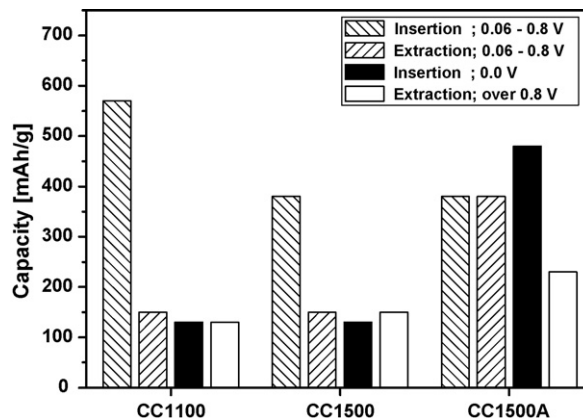


Fig. 5. The first cycle charge/discharge capacity changes of CC1100, CC1500, and CC1500A.

migrate effectively under these carbonization conditions, which makes the complete removal of iron oxides difficult.

Note also that Li insertion at ~ 0.00 V is considerably higher in CC1500A (480 mAh/g) than in both CC1100 and CC1500 (130 mAh/g), but that the discharge capacity at ~ 0.00 V is almost the same, ~ 10 mAh/g for all samples. This implies that Li ions can be more effectively stored in a larger number of smaller pores, but that the differences between the average pore diameters of the samples, i.e. ~ 60 nm for CC1100 and CC1500 and ~ 6 nm for CC1500A, influence the discharge energy barrier of the Li ions very little.

By examining the quantitative changes in the charge and discharge capacities of CC1100, CC1500, and CC1500A in the various voltage ranges in Fig. 5, we can see that in the 0.06–0.80 V region, CC1500A exhibits $\sim 100\%$ efficiency in the insertion/extraction of Li ions with a stable capacity of ~ 400 mAh/g. This is in contrast to the cases of CC1100 and CC1500, for which there are large irreversible charge/discharge behaviors in this voltage region. This result confirms that the microtexture of CC1500A, characterized by a web-like open framework structure consisting of highly crystalline and highly crimped carbon nanofibrils, results in highly efficient Li-ion insertion/extraction processes.

The irreversible capacity is the difference between the charge capacity at 0.0 V and the discharge capacity over 0.8 V and can be a measure of the surface reactions occurring during the adsorption/desorption of Li ions on the surfaces of the carbon layers. Considering the structural differences between CC1100 and CC1500, the remarkably decreased irreversibility of CC1500 is probably because the number of surface reaction sites, i.e. the number of edge carbons, is much reduced in CC1500. However, that the irreversibility of CC1500A is higher than that of CC1500 cannot be explained in such terms because CC1500A is expected to have many fewer edge carbons than its unannealed counterpart. This result is possibly due to the chemical nature of the edge carbons. Radovic and Bockrath [19] recently concluded from experimental observations and a theoretical study of the chemical nature of the edge carbons in a graphene layer that two different chemical states can be differentiated even in the absence of heteroatoms such as H, N,

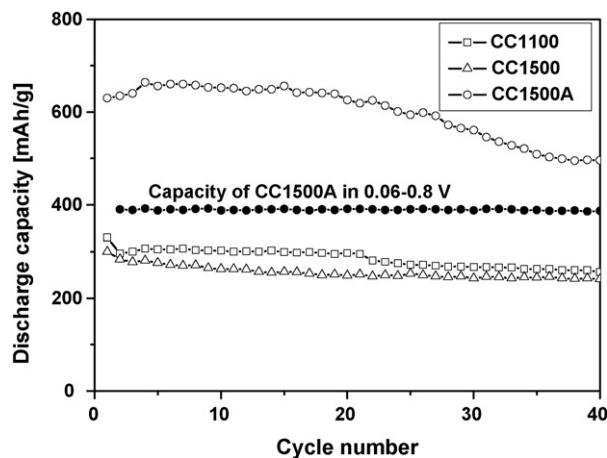


Fig. 6. Cycle performances of CC1100, CC1500, and CC1500A.

O, etc.; in a highly developed graphene layer, the zigzag type edge carbons are carbene-like, with the triplet ground state the most common (the pairing of electrons), and the armchair type edge carbons are carbyne-like, with the singlet ground state the most common. This claim remains in dispute but it is generally agreed that the carbyne-like species are more stable than the carbene-like species. Thus, the higher irreversible capacity of the CC1500A sample might be due to a higher number of reactive carbene-like species at the peripheries of the carbon layers, which result from the annealing process [20].

Fig. 6 shows the cycle behaviors of CC1100, CC1500, and CC1500A. The discharge capacities of all the samples gradually decrease from the first to the 40th cycle after which they remain nearly constant. In the case of CC1500A, the discharge capacity increases up to the 4th cycle and then gradually decreases. The first increase in the capacity appears to reflect a kind of capacitor effect due to the presence of nanopores, although the exact reason for this increase is not clear at this stage.

The electrochemical performance of CC1500A is much superior to those of the most recently reported nano-carbon anode materials, as shown in Fig. 7. For example, highly crystalline carbon nanofibers fabricated with a catalytic chemical vapor deposition method [21] were found to exhibit a capacity of

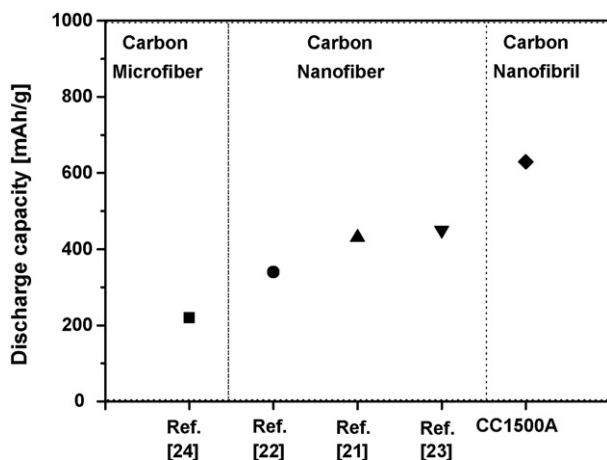


Fig. 7. Discharge capacities of various carbon anode materials and CC1500A.

431 mAh/g, and other carbon nanofibers produced in a high dc field were found to have a capacity of 340 mAh/g [22]. Carbon nanofiber webs derived from electrospinning were reported to have a capacity of approximately 450 mAh/g [23]. In contrast, micro-sized PAN carbon fibers were reported to have a capacity of approximately 220 mAh/g [24]. These results confirm that the microtextural features of CC1500A, i.e. the shorter diffusion paths due to its nanofibrillar nature, its high crystallinity, highly crimped nanofibrils, and open framework structure, obviously result in enhanced anodic performance in lithium-ion batteries. However, it is noteworthy that, when the bulk density (0.98 g/cm^3) of CC1500A was considered, the volumetric capacity of CC1500A turned out to be somewhat lower (approximately 620 mAh/cm^3) than the theoretical volumetric capacity of the ideal graphite (830 mAh/cm^3) [25].

4. Conclusions

A novel carbon anode with a microtexture characterized by a web-like open framework structure consisting of highly crystalline and highly crimped carbon nanofibrils (denoted ‘carbon-cotton’) was prepared via the simple solid-phase carbonization of PAN/FeCl₃ hybrid precursor, and its anodic performance was tested. The carbon-cottons and in particular the thermally annealed sample, CC1500A, were found to have excellent anodic performances, such as a very good rechargeable capacity of $\sim 630 \text{ mAh/g}$ with a Coulomb efficiency of $\sim 70\%$, and very stable cycling behavior up to the experimentally tested maximum number of 40 cycles. The excellent anodic performance of CC1500A is due to its microtextural features, i.e. the web-like open framework structure consisting of highly crystalline and highly crimped carbon nanofibrils; this kind of microtexture is expected to have high resilience to volume deformation of the anode during the Li-ion insertion/extraction process. Indeed, our results confirm this expectation: the charge/discharge efficiency of $\sim 100\%$ in the range 0.06–0.80 V indicates that the carbon-cotton undergoes a completely elastic recovery from the large volume deformation that occurs during Li-ion insertion/extraction.

References

- [1] S. Iijima, Nature 354 (1991) 56.
- [2] K. Komatsu, M. Murata, Y. Murata, Science 207 (2005) 238.
- [3] J. Lee, S. Yoon, S.M. Oh, C. Shin, T.H. Hyeon, Adv. Mater. 12 (2000) 359.
- [4] G. Che, B.B. Lakshmi, E.R. Fisher, C.R. Martin, Nature 393 (1998) 346.
- [5] J. Jang, B. Lim, Adv. Mater. 14 (2002) 1390.
- [6] B. Gao, A. Kleinhammes, X.P. Tang, C. Bower, L. Fleming, Y. Wu, O. Zhou, Chem. Phys. Lett. 307 (1999) 153.
- [7] T.P. Kumar, R. Ramesh, Y.Y. Lin, G.T.K. Fey, Electrochem. Commun. 6 (2004) 520.
- [8] Y.-P. Wu, C.-R. Wan, C.-Y. Jiang, S.-B. Fang, Y.-Y. Jiang, Carbon 37 (1999) 1901.
- [9] A. Mabuchi, K. Tokumitsu, H. Fujimoto, T. Kasuh, Electrochem. Soc. 142 (1995) 1041.
- [10] Y.J. Kim, C.R. Park, Inorg. Chem. 41 (2002) 6211.
- [11] Y.P. Wu, E. Rahm, R. Holze, J. Power Sources 114 (2003) 228.
- [12] T.W. Ebbesen, Carbon Nanotubes; Preparation and Properties, CRC Press, Boca Raton, 1997.

- [13] A. Oberlin, in: P.A. Throver (Ed.), *Chemistry and Physics of Carbon: High Resolution TEM Studies of Carbonization and Graphitization*, vol. 22, Dekker, New York, 1989.
- [14] J.N. Rouzaud, A. Oberlin, *Carbon* 27 (1989) 517.
- [15] E. Buiel, J.R. Dahn, *Electrochim. Acta* 45 (1999) 121.
- [16] G. Li, R. Xue, L. Chen, Y.Z. Huang, *J. Power Sources* 54 (1995) 271.
- [17] I. Mochida, C.H. Ku, S.H. Yoon, Y. Korai, *J. Power Sources* 75 (1998) 214.
- [18] S.H. Yoon, S. Lim, S.H. Hong, I. Mochida, B. An, K. Yokogawa, *Carbon* 42 (2004) 3087.
- [19] L. Radovic, B. Bockrath, *J. Am. Chem. Soc.* 127 (2005) 5917.
- [20] S. Shiraishi, T. Kobayashi, A. Oya, *Chem. Lett.* 34 (2005) 1678.
- [21] S.H. Yoon, C.W. Park, H.J. Yang, Y. Korai, I. Mochida, R.T.K. Baker, N.M. Rodriguez, *Carbon* 42 (2004) 21.
- [22] T. Doi, A. Fukuda, Y. Iriyama, T. Abe, Z. Ogumi, K. Nakagawa, T. Ando, *Electrochem. Commun.* 7 (2005) 10.
- [23] C. Kim, K.S. Yang, M. Kojima, K. Yoshida, Y.J. Kim, Y.A. Kim, M. Endo, *Adv. Funct. Mater.* 16 (2006) 2393.
- [24] J.K. Lee, K.W. An, J.B. Ju, B.W. Cho, W.I. Cho, D. Park, K.S. Yun, *Carbon* 39 (2001) 1299.
- [25] M. Yoshio, H. Wang, K. Fukuda, T. Umeno, N. Dimov, Z. Ogumi, *J. Electrochem. Soc.* 149 (2002) A1598.